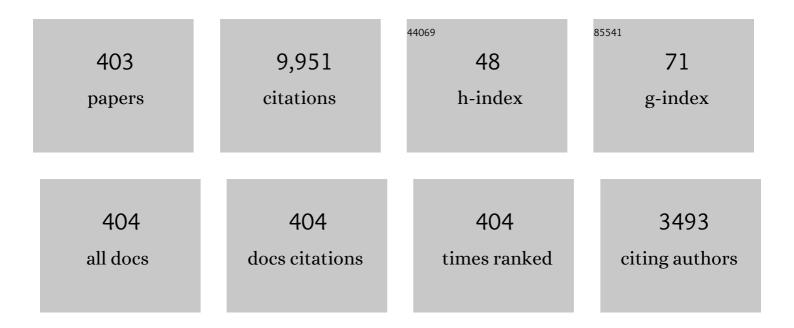
Marco Wischmeier

List of Publications by Year in descending order

Source: https://exaly.com/author-pdf/3863218/publications.pdf Version: 2024-02-01



#	Article	IF	CITATIONS
1	Predictions of radiation pattern and in–out asymmetries in the DEMO scrape-off layer using fluid neutrals. Nuclear Fusion, 2022, 62, 056015.	3.5	4
2	Experimental investigation of L- and H-mode detachment via the divertor Thomson scattering at ASDEX Upgrade. Nuclear Fusion, 2022, 62, 066027.	3.5	8
3	Plasma physics and control studies planned in JT-60SA for ITER and DEMO operations and risk mitigation. Plasma Physics and Controlled Fusion, 2022, 64, 054004.	2.1	6
4	Overview of the TCV tokamak experimental programme. Nuclear Fusion, 2022, 62, 042018.	3.5	30
5	Towards assessment of plasma edge transport in Neon seeded plasmas in disconnected double null configuration in EAST with SOLPS-ITER. Nuclear Materials and Energy, 2021, 26, 100926.	1.3	2
6	Study of detachment in future ASDEX Upgrade alternative divertor configurations by means of EMC3-EIRENE. Nuclear Materials and Energy, 2021, 26, 100950.	1.3	4
7	Assessment of Scrape-Off Layer and divertor plasma conditions in JT-60SA with tungsten wall and nitrogen injection. Nuclear Materials and Energy, 2021, 26, 100895.	1.3	5
8	Scoping the characteristics and benefits of a connected double-null configuration for power exhaust in EU-DEMO. Nuclear Materials and Energy, 2021, 26, 100886.	1.3	6
9	Preliminary analysis of alternative divertors for DEMO. Nuclear Materials and Energy, 2021, 26, 100908.	1.3	19
10	The operational space for divertor power exhaust in DEMO with a super-X divertor. Nuclear Fusion, 2021, 61, 076007.	3.5	7
11	Numerical modelling of an enhanced perpendicular transport regime in the scrape-off layer of ASDEX Upgrade. Plasma Physics and Controlled Fusion, 2021, 63, 075003.	2.1	12
12	SOLPS-ITER validation with TCV L-mode discharges. Physics of Plasmas, 2021, 28, 082508.	1.9	9
13	SOLPS-ITER modeling of ASDEX Upgrade L-mode detachment states. Plasma Physics and Controlled Fusion, 2021, 63, 105005.	2.1	8
14	Parameter dependencies of the experimental nitrogen concentration required for detachment on ASDEX Upgrade and JET. Nuclear Materials and Energy, 2021, 28, 101000.	1.3	2
15	Developments towards an ELM-free pedestal radiative cooling scenario using noble gas seeding in ASDEX Upgrade. Nuclear Fusion, 2021, 61, 016002.	3.5	33
16	X-point radiation, its control and an ELM suppressed radiating regime at the ASDEX Upgrade tokamak. Nuclear Fusion, 2021, 61, 024001.	3.5	59
17	Experimental verification of X-point potential well formation in unfavorable magnetic field direction. Nuclear Materials and Energy, 2020, 25, 100839.	1.3	7
18	X-point potential well formation in diverted tokamaks with unfavorable magnetic field direction. Nuclear Fusion, 2020, 60, 054005.	3.5	24

#	Article	IF	CITATIONS
19	Self-sustained divertor oscillations in ASDEX Upgrade. Nuclear Fusion, 2020, 60, 076013.	3.5	7
20	Summary of the 3rd IAEA technical meeting on divertor concepts. Nuclear Fusion, 2020, 60, 097001.	3.5	2
21	Peculiarity of highly radiating multi-impurity seeded <i>H</i> -mode plasmas on JET with ITER-like wall. Physica Scripta, 2020, T171, 014055.	2.5	10
22	Shaping effects on scrape-off layer plasma turbulence: A rigorous validation of three-dimensional simulations against TCV measurements. Physics of Plasmas, 2020, 27, .	1.9	10
23	H-mode confinement in the pellet-enforced high-density regime of the all-metal-wall tokamak ASDEX Upgrade. Nuclear Fusion, 2020, 60, 092003.	3.5	9
24	Comparison of SOLPS5.0 and SOLPSâ€ITER simulations for ASDEX upgrade Lâ€node. Contributions To Plasma Physics, 2020, 60, e201900120.	1.1	2
25	Advances in the physics studies for the JT-60SA tokamak exploitation and research plan. Plasma Physics and Controlled Fusion, 2020, 62, 014009.	2.1	18
26	SOLPS-ITER modeling with activated drifts for a snowflake divertor in ASDEX Upgrade. Plasma Physics and Controlled Fusion, 2020, 62, 045005.	2.1	15
27	The diffusion limit of ballistic transport in the scrape-off layer. Physics of Plasmas, 2020, 27, .	1.9	11
28	Impact of drifts in the ASDEX upgrade upper open divertor using SOLPSâ€ITER. Contributions To Plasma Physics, 2020, 60, e201900166.	1.1	5
29	Impurity transport and divertor retention in Ar and N seeded SOLPS 5.0 simulations for ASDEX Upgrade. Plasma Physics and Controlled Fusion, 2020, 62, 085013.	2.1	18
30	Near- and far scrape-off layer transport studies in detached, small-ELM ASDEX Upgrade discharges by means of EMC3-EIRENE. Plasma Physics and Controlled Fusion, 2020, 62, 105016.	2.1	8
31	Measuring fast ions in fusion plasmas with neutron diagnostics at JET. Plasma Physics and Controlled Fusion, 2019, 61, 014027.	2.1	23
32	Overview of physics studies on ASDEX Upgrade. Nuclear Fusion, 2019, 59, 112014.	3.5	38
33	Novel method for determination of tritium depth profiles in metallic samples. Nuclear Fusion, 2019, 59, 106006.	3.5	2
34	Langmuir probe electronics upgrade on the tokamak à configuration variable. Review of Scientific Instruments, 2019, 90, 083502.	1.3	26
35	Isotope identity experiments in JET-ILW with H and D L-mode plasmas. Nuclear Fusion, 2019, 59, 076028.	3.5	31
36	Role of the pedestal position on the pedestal performance in AUG, JET-ILW and TCV and implications for ITER. Nuclear Fusion, 2019, 59, 076038.	3.5	43

#	Article	IF	CITATIONS
37	A new mechanism for increasing density peaking in tokamaks: improvement of the inward particle pinch with edge <i>E</i> × <i>B</i> shearing. Plasma Physics and Controlled Fusion, 2019, 61, 104002.	2.1	12
38	SOLPS-ITER simulations of the TCV divertor upgrade. Plasma Physics and Controlled Fusion, 2019, 61, 085029.	2.1	35
39	Erosion, screening, and migration of tungsten in the JET divertor. Nuclear Fusion, 2019, 59, 096035.	3.5	60
40	EDGE2D-EIRENE simulations of the influence of isotope effects and anomalous transport coefficients on near scrape-off layer radial electric field. Plasma Physics and Controlled Fusion, 2019, 61, 075010.	2.1	11
41	Characterisation of highly radiating neon seeded plasmas in JET-ILW. Nuclear Fusion, 2019, 59, 126031.	3.5	37
42	Synthetic diagnostic for the JET scintillator probe lost alpha measurements. Journal of Instrumentation, 2019, 14, C09018-C09018.	1.2	0
43	Self-consistent pedestal prediction for JET-ILW in preparation of the DT campaign. Physics of Plasmas, 2019, 26, .	1.9	26
44	Interpretative and predictive modelling of Joint European Torus collisionality scans. Plasma Physics and Controlled Fusion, 2019, 61, 115004.	2.1	4
45	Physics research on the TCV tokamak facility: from conventional to alternative scenarios and beyond. Nuclear Fusion, 2019, 59, 112023.	3.5	43
46	A machine learning approach based on generative topographic mapping for disruption prevention and avoidance at JET. Nuclear Fusion, 2019, 59, 106017.	3.5	36
47	Determination of isotope ratio in the divertor of JET-ILW by high-resolution H <i>α</i> spectroscopy: H–D experiment and implications for D–T experiment. Nuclear Fusion, 2019, 59, 046011.	3.5	23
48	Modelling of tungsten erosion and deposition in the divertor of JET-ILW in comparison to experimental findings. Nuclear Materials and Energy, 2019, 18, 239-244.	1.3	24
49	A locked mode indicator for disruption prediction on JET and ASDEX upgrade. Fusion Engineering and Design, 2019, 138, 254-266.	1.9	8
50	Dependence on plasma shape and plasma fueling for small edge-localized mode regimes in TCV and ASDEX Upgrade. Nuclear Fusion, 2019, 59, 086020.	3.5	34
51	Impact of fast ions on density peaking in JET: fluid and gyrokinetic modeling. Plasma Physics and Controlled Fusion, 2019, 61, 075008.	2.1	3
52	Diagnostic of fast-ion energy spectra and densities in magnetized plasmas. Journal of Instrumentation, 2019, 14, C05019-C05019.	1.2	12
53	Assessment of particle and heat loads to the upper open divertor in ASDEX Upgrade in favourable and unfavourable toroidal magnetic field directions. Nuclear Materials and Energy, 2019, 19, 531-536.	1.3	4
54	Overview of the JET preparation for deuterium–tritium operation with the ITER like-wall. Nuclear Fusion, 2019, 59, 112021.	3.5	87

#	Article	IF	CITATIONS
55	An assessment of nitrogen concentrations from spectroscopic measurements in the JET and ASDEX upgrade divertor. Nuclear Materials and Energy, 2019, 18, 147-152.	1.3	8
56	Effect of magnetic perturbation fields on power decay length in EMC3-EIRENE simulations and comparison to experiment in ASDEX upgrade. Nuclear Materials and Energy, 2019, 19, 205-210.	1.3	2
57	Adaptive learning for disruption prediction in non-stationary conditions. Nuclear Fusion, 2019, 59, 086037.	3.5	27
58	2D and 3D studies of the X-divertor configuration in the future upper divertor of ASDEX upgrade. Nuclear Materials and Energy, 2019, 19, 107-112.	1.3	5
59	COREDIV numerical simulation of high neutron rate JET-ILW DD pulses in view of extension to JET-ILW DT experiments. Nuclear Fusion, 2019, 59, 056026.	3.5	4
60	SOLPS 5.0 simulations of the high-field side divertor detachment of L-mode plasmas in ASDEX upgrade with convection-dominated radial SOL transport. Nuclear Materials and Energy, 2019, 19, 279-286.	1.3	2
61	Tritium distributions on W-coated divertor tiles used in the third JET ITER-like wall campaign. Nuclear Materials and Energy, 2019, 18, 258-261.	1.3	10
62	Evolution of nitrogen concentration and ammonia production in N ₂ -seeded H-mode discharges at ASDEX Upgrade. Nuclear Fusion, 2019, 59, 046010.	3.5	22
63	Real-time plasma state monitoring and supervisory control on TCV. Nuclear Fusion, 2019, 59, 026017.	3.5	13
64	Validation of the ICRF antenna coupling code RAPLICASOL against TOPICA and experiments. Nuclear Fusion, 2019, 59, 046001.	3.5	31
65	Population modelling of the He II energy levels in tokamak plasmas: I. Collisional excitation model. Journal of Physics B: Atomic, Molecular and Optical Physics, 2019, 52, 045001.	1.5	1
66	Radial variation of heat transport in L-mode JET discharges. Nuclear Fusion, 2019, 59, 056006.	3.5	3
67	Micro ion beam analysis for the erosion of beryllium marker tiles in a tokamak limiter. Nuclear Instruments & Methods in Physics Research B, 2019, 450, 200-204.	1.4	1
68	ELM-induced cold pulse propagation in ASDEX Upgrade. Plasma Physics and Controlled Fusion, 2019, 61, 045003.	2.1	6
69	Analysis of deposited layers with deuterium and impurity elements on samples from the divertor of JET with ITER-like wall. Journal of Nuclear Materials, 2019, 516, 202-213.	2.7	18
70	Analysis of the outer divertor hot spot activity in the protection video camera recordings at JET. Fusion Engineering and Design, 2019, 139, 115-123.	1.9	3
71	Improved neutron activation dosimetry for fusion. Fusion Engineering and Design, 2019, 139, 109-114.	1.9	7
72	Full-orbit and drift calculations of fusion product losses due to explosive fishbones on JET. Nuclear Fusion, 2019, 59, 016004.	3.5	9

#	Article	IF	CITATIONS
73	Effect of magnetic perturbations for ELM control on divertor power loads, detachment and consequences of field penetration in ASDEX Upgrade. Plasma Physics and Controlled Fusion, 2019, 61, 014008.	2.1	8
74	Adaptive predictors based on probabilistic SVM for real time disruption mitigation on JET. Nuclear Fusion, 2018, 58, 056002.	3.5	44
75	Scenario development for the observation of alpha-driven instabilities in JET DT plasmas. Nuclear Fusion, 2018, 58, 082005.	3.5	34
76	A multi-machine scaling of halo current rotation. Nuclear Fusion, 2018, 58, 016050.	3.5	18
77	Plasma-wall interaction on the divertor tiles of JET ITER-like wall from the viewpoint of micro/nanoscopic observations. Fusion Engineering and Design, 2018, 136, 199-204.	1.9	5
78	Correlation of the tokamak H-mode density limit with ballooning stability at the separatrix. Nuclear Fusion, 2018, 58, 034001.	3.5	57
79	Neutron spectroscopy measurements of 14 MeV neutrons at unprecedented energy resolution and implications for deuterium–tritium fusion plasma diagnostics. Measurement Science and Technology, 2018, 29, 045502.	2.6	35
80	Versatile fusion source integrator AFSI for fast ion and neutron studies in fusion devices. Nuclear Fusion, 2018, 58, 016023.	3.5	17
81	Light impurity transport in JET ILW L-mode plasmas. Nuclear Fusion, 2018, 58, 036009.	3.5	13
82	14 MeV calibration of JET neutron detectors—phase 1: calibration and characterization of the neutron source. Nuclear Fusion, 2018, 58, 026012.	3.5	22
83	ERO modeling and sensitivity analysis of locally enhanced beryllium erosion by magnetically connected antennas. Nuclear Fusion, 2018, 58, 016046.	3.5	9
84	Bayesian Integrated Data Analysis of Fast-Ion Measurements by Velocity-Space Tomography. Fusion Science and Technology, 2018, 74, 23-36.	1.1	15
85	lsotope effects on L-H threshold and confinement in tokamak plasmas. Plasma Physics and Controlled Fusion, 2018, 60, 014045.	2.1	98
86	Divertor, scrape-off layer and pedestal particle dynamics in the ELM cycle on ASDEX Upgrade. Plasma Physics and Controlled Fusion, 2018, 60, 025002.	2.1	12
87	Investigation into the formation of the scrape-off layer density shoulder in JET ITER-like wall L-mode and H-mode plasmas. Nuclear Fusion, 2018, 58, 056001.	3.5	38
88	High Z neoclassical transport: Application and limitation of analytical formulae for modelling JET experimental parameters. Physics of Plasmas, 2018, 25, .	1.9	14
89	Poloidal asymmetries in the edge density profiles on ASDEX Upgrade. Nuclear Fusion, 2018, 58, 026005.	3.5	11
90	Escaping alpha-particle monitor for burning plasmas. Nuclear Fusion, 2018, 58, 082009.	3.5	3

#	Article	IF	CITATIONS
91	On the universality of power laws for tokamak plasma predictions. Plasma Physics and Controlled Fusion, 2018, 60, 025028.	2.1	8
92	SOLPS simulations of detachment in a snowflake configuration for the future upper divertor in ASDEX Upgrade. Plasma Physics and Controlled Fusion, 2018, 60, 085005.	2.1	16
93	Tritium retention characteristics in dust particles in JET with ITER-like wall. Nuclear Materials and Energy, 2018, 17, 279-283.	1.3	20
94	Application of the VUV and the soft x-ray systems on JET for the study of intrinsic impurity behavior in neon seeded hybrid discharges. Review of Scientific Instruments, 2018, 89, 10D131.	1.3	4
95	3D non-linear MHD simulation of the MHD response and density increase as a result of shattered pellet injection. Nuclear Fusion, 2018, 58, 126025.	3.5	29
96	Application of the Denovo Discrete Ordinates Radiation Transport Code to Large-Scale Fusion Neutronics. Fusion Science and Technology, 2018, 74, 303-314.	1.1	5
97	Dependence of the turbulent particle flux on hydrogen isotopes induced by collisionality. Physics of Plasmas, 2018, 25, 082517.	1.9	16
98	On the role of finite grid extent in SOLPS-ITER edge plasma simulations for JET H-mode discharges with metallic wall. Nuclear Materials and Energy, 2018, 17, 174-181.	1.3	8
99	Effects of nitrogen seeding on core ion thermal transport in JET ILW L-mode plasmas. Nuclear Fusion, 2018, 58, 026028.	3.5	17
100	Determination of 2D poloidal maps of the intrinsic W density for transport studies in JET-ILW. Review of Scientific Instruments, 2018, 89, 113501.	1.3	13
101	Real-time-capable prediction of temperature and density profiles in a tokamak using RAPTOR and a first-principle-based transport model. Nuclear Fusion, 2018, 58, 096006.	3.5	41
102	On the role of filaments in perpendicular heat transport at the scrape-off layer. Nuclear Fusion, 2018, 58, 096015.	3.5	41
103	Propagating transport-code input parameter uncertainties with deterministic sampling. Plasma Physics and Controlled Fusion, 2018, 60, 125010.	2.1	0
104	Synthetic spectra of BeH, BeD and BeT for emission modeling in JET plasmas. Journal of Physics B: Atomic, Molecular and Optical Physics, 2018, 51, 185701.	1.5	17
105	Assessment of the strength of kinetic effects of parallel electron transport in the SOL and divertor of JET high radiative H-mode plasmas using EDGE2D-EIRENE and KIPP codes. Plasma Physics and Controlled Fusion, 2018, 60, 115011.	2.1	12
106	First principles of modelling the stabilization of microturbulence by fast ions. Nuclear Fusion, 2018, 58, 082024.	3.5	22
107	Impact of electron-scale turbulence and multi-scale interactions in the JET tokamak. Nuclear Fusion, 2018, 58, 124003.	3.5	23
108	Generation of a plasma neutron source for Monte Carlo neutron transport calculations in the tokamak JET. Fusion Engineering and Design, 2018, 136, 1047-1051.	1.9	9

#	Article	IF	CITATIONS
109	Observation of enhanced ion particle transport in mixed H/D isotope plasmas on JET. Nuclear Fusion, 2018, 58, 076022.	3.5	20
110	Fast H isotope and impurity mixing in ion-temperature-gradient turbulence. Nuclear Fusion, 2018, 58, 076028.	3.5	33
111	W transport and accumulation control in the termination phase of JET H-mode discharges and implications for ITER. Plasma Physics and Controlled Fusion, 2018, 60, 074008.	2.1	26
112	Neutral pathways and heat flux widths in vertical- and horizontal-target EDGE2D-EIRENE simulations of JET. Nuclear Fusion, 2018, 58, 096029.	3.5	19
113	Molecular ND Band Spectroscopy in the Divertor Region of Nitrogen Seeded JET Discharges. Journal of Physics: Conference Series, 2018, 959, 012009.	0.4	7
114	Review of recent experimental and modeling advances in the understanding of lower hybrid current drive in ITER-relevant regimes. Nuclear Fusion, 2018, 58, 095003.	3.5	16
115	Integrated modelling of H-mode pedestal and confinement in JET-ILW. Plasma Physics and Controlled Fusion, 2018, 60, 014042.	2.1	40
116	Scaling of the geodesic acoustic mode amplitude on JET. Plasma Physics and Controlled Fusion, 2018, 60, 085006.	2.1	5
117	First principle integrated modeling of multi-channel transport including Tungsten in JET. Nuclear Fusion, 2018, 58, 096003.	3.5	22
118	Alpha heating, isotopic mass, and fast ion effects in deuterium–tritium experiments. Nuclear Fusion, 2018, 58, 096011.	3.5	3
119	Stability and propagation of the high field side high density front in the fluctuating state of detachment in ASDEX Upgrade. Nuclear Materials and Energy, 2017, 12, 1152-1156.	1.3	9
120	High power neon seeded JET discharges: Experiments and simulations. Nuclear Materials and Energy, 2017, 12, 882-886.	1.3	13
121	Assessment of erosion, deposition and fuel retention in the JET-ILW divertor from ion beam analysis data. Nuclear Materials and Energy, 2017, 12, 559-563.	1.3	28
122	Beryllium film deposition in cavity samples in remote areas of the JET divertor during the 2011–2012 ITER-like wall campaign. Nuclear Materials and Energy, 2017, 12, 548-552.	1.3	14
123	Energy balance in JET. Nuclear Materials and Energy, 2017, 12, 227-233.	1.3	18
124	Possible influence of near SOL plasma on the H-mode power threshold. Nuclear Materials and Energy, 2017, 12, 273-277.	1.3	16
125	Detachment evolution on the TCV tokamak. Nuclear Materials and Energy, 2017, 12, 1071-1076.	1.3	37
126	Gyrokinetic study of turbulent convection of heavy impurities in tokamak plasmas at comparable ion and electron heat fluxes. Nuclear Fusion, 2017, 57, 022009.	3.5	27

#	Article	IF	CITATIONS
127	Progress in understanding disruptions triggered by massive gas injection via 3D non-linear MHD modelling with JOREK. Plasma Physics and Controlled Fusion, 2017, 59, 014006.	2.1	47
128	Studies of dust from JET with the ITER-Like Wall: Composition and internal structure. Nuclear Materials and Energy, 2017, 12, 582-587.	1.3	41
129	Plasma impact on diagnostic mirrors in JET. Nuclear Materials and Energy, 2017, 12, 506-512.	1.3	25
130	Assessment of SOLPS5.0 divertor solutions with drifts and currents against L-mode experiments in ASDEX Upgrade and JET. Plasma Physics and Controlled Fusion, 2017, 59, 035003.	2.1	27
131	Generation of the neutron response function of an NE213 scintillator for fusion applications. Nuclear Instruments and Methods in Physics Research, Section A: Accelerators, Spectrometers, Detectors and Associated Equipment, 2017, 866, 222-229.	1.6	5
132	Plasma edge and plasma-wall interaction modelling: Lessons learned from metallic devices. Nuclear Materials and Energy, 2017, 12, 3-17.	1.3	17
133	Impact of the JET ITER-like wall on H-mode plasma fueling. Nuclear Fusion, 2017, 57, 066024.	3.5	6
134	Efficient generation of energetic ions in multi-ion plasmas by radio-frequency heating. Nature Physics, 2017, 13, 973-978.	16.7	73
135	Ion cyclotron resonance heating for tungsten control in various JET H-mode scenarios. Plasma Physics and Controlled Fusion, 2017, 59, 055001.	2.1	32
136	Classification of ELM types in Joint European Torus based on global plasma parameters using discriminant analysis. Fusion Engineering and Design, 2017, 123, 717-721.	1.9	1
137	Simulation of neutral gas flow in the JET sub-divertor. Fusion Engineering and Design, 2017, 121, 13-21.	1.9	20
138	The effect of the isotope on the H-mode density limit. Nuclear Fusion, 2017, 57, 086007.	3.5	9
139	TCV divertor upgrade for alternative magnetic configurations. Nuclear Materials and Energy, 2017, 12, 1106-1111.	1.3	26
140	The emissivity of W coatings deposited on carbon materials for fusion applications. Fusion Engineering and Design, 2017, 114, 192-195.	1.9	9
141	Micro-/nano-characterization of the surface structures on the divertor tiles from JET ITER-like wall. Fusion Engineering and Design, 2017, 116, 1-4.	1.9	14
142	CeBr3–based detector for gamma-ray spectrometer upgrade at JET. Fusion Engineering and Design, 2017, 123, 986-989.	1.9	4
143	Expanding the role of impurity spectroscopy for investigating the physics of high-Z dissipative divertors. Nuclear Materials and Energy, 2017, 12, 91-99.	1.3	7
144	Overview of the JET ITER-like wall divertor. Nuclear Materials and Energy, 2017, 12, 499-505.	1.3	46

#	Article	IF	CITATIONS
145	Power exhaust by SOL and pedestal radiation at ASDEX Upgrade and JET. Nuclear Materials and Energy, 2017, 12, 111-118.	1.3	92
146	Proposal of an alternative upper divertor in ASDEX Upgrade supported by EMC3-EIRENE simulations. Nuclear Materials and Energy, 2017, 12, 1037-1042.	1.3	23
147	The high field side high density region in SOLPS-modeling of nitrogen-seeded H-modes in ASDEX Upgrade. Nuclear Materials and Energy, 2017, 12, 193-199.	1.3	77
148	Main chamber wall plasma loads in JET-ITER-like wall at high radiated fraction. Nuclear Materials and Energy, 2017, 12, 234-240.	1.3	7
149	Modeling of argon seeding in ASDEX Upgrade H-mode plasma with SOLPS5.0. Nuclear Materials and Energy, 2017, 12, 1146-1151.	1.3	3
150	Structure, tritium depth profile and desorption from â€~plasma-facing' beryllium materials of ITER-Like-Wall at JET. Nuclear Materials and Energy, 2017, 12, 642-647.	1.3	14
151	3D simulations of gas puff effects on edge plasma and ICRF coupling in JET. Nuclear Fusion, 2017, 57, 056042.	3.5	14
152	Determining the prediction limits of models and classifiers with applications for disruption prediction in JET. Nuclear Fusion, 2017, 57, 016024.	3.5	4
153	Comparative H-mode density limit studies in JET and AUG. Nuclear Materials and Energy, 2017, 12, 100-110.	1.3	13
154	The effect of lower hybrid waves on JET plasma rotation. Nuclear Fusion, 2017, 57, 034002.	3.5	6
155	Investigation of the effects of impurity seeding under different magnetic configurations in L-mode plasma in EAST tokamak. Physics of Plasmas, 2017, 24, 092514.	1.9	9
156	Investigation of sustainable high-βscenarios in the JT-60SA C-wall. Nuclear Fusion, 2017, 57, 116010.	3.5	4
157	Velocity-space sensitivities of neutron emission spectrometers at the tokamaks JET and ASDEX Upgrade in deuterium plasmas. Review of Scientific Instruments, 2017, 88, 073506.	1.3	30
158	A tool to support the construction of reliable disruption databases. Fusion Engineering and Design, 2017, 125, 139-153.	1.9	12
159	Overview of progress in European medium sized tokamaks towards an integrated plasma-edge/wall solution ^a . Nuclear Fusion, 2017, 57, 102014.	3.5	23
160	Towards self-consistent plasma modelisation in presence of neoclassical tearing mode and sawteeth: effects on transport coefficients. Plasma Physics and Controlled Fusion, 2017, 59, 125012.	2.1	2
161	Evaluation of the plasma hydrogen isotope content by residual gas analysis at JET and AUG. Physica Scripta, 2017, T170, 014021.	2.5	6
162	Simulation of JET ITER-Like Wall pulses at high neon seeding rate. Nuclear Fusion, 2017, 57, 126021.	3.5	10

#	Article	IF	CITATIONS
163	Real-time control of divertor detachment in H-mode with impurity seeding using Langmuir probe feedback in JET-ITER-like wall. Plasma Physics and Controlled Fusion, 2017, 59, 045001.	2.1	43
164	Dynamics and stability of divertor detachment in H-mode plasmas on JET. Plasma Physics and Controlled Fusion, 2017, 59, 095003.	2.1	34
165	Quartz micro-balance results of pulse-resolved erosion/deposition in the JET-ILW divertor. Nuclear Materials and Energy, 2017, 12, 478-482.	1.3	6
166	ELM divertor peak energy fluence scaling to ITER with data from JET, MAST and ASDEX upgrade. Nuclear Materials and Energy, 2017, 12, 84-90.	1.3	116
167	Development of MPPC-based detectors for high count rate DT campaigns at JET. Fusion Engineering and Design, 2017, 123, 940-944.	1.9	5
168	Real time control developments at JET in preparation for deuterium-tritium operation. Fusion Engineering and Design, 2017, 123, 535-540.	1.9	7
169	SOL parallel momentum loss in ASDEX Upgrade and comparison with SOLPS. Nuclear Materials and Energy, 2017, 12, 181-186.	1.3	18
170	Overview of the JET results in support to ITER. Nuclear Fusion, 2017, 57, 102001.	3.5	150
171	An optimized upper divertor with divertor-coils to study enhanced divertor configurations in ASDEX Upgrade. Fusion Engineering and Design, 2017, 123, 508-512.	1.9	9
172	Determination of the stochastic layer properties induced by magnetic perturbations via heat pulse experiments at ASDEX upgrade. Nuclear Materials and Energy, 2017, 12, 831-837.	1.3	5
173	Gyrokinetic simulations of particle transport in pellet fuelled JET discharges. Plasma Physics and Controlled Fusion, 2017, 59, 105005.	2.1	2
174	Sawtooth pacing with on-axis ICRH modulation in JET-ILW. Nuclear Fusion, 2017, 57, 036027.	3.5	23
175	Impact of divertor geometry on H-mode confinement in the JET metallic wall. Nuclear Fusion, 2017, 57, 086025.	3.5	24
176	Modelling of transitions between L- and H-mode in JET high plasma current plasmas and application to ITER scenarios including tungsten behaviour. Nuclear Fusion, 2017, 57, 086023.	3.5	22
177	Analysis of activation and damage of ITER material samples expected from DD/DT campaign at JET. Fusion Engineering and Design, 2017, 125, 307-313.	1.9	6
178	EDGE2D-EIRENE simulations of the impact of poloidal flux expansion on the radiative divertor performance in JET. Nuclear Materials and Energy, 2017, 12, 786-790.	1.3	3
179	Assessment of divertor heat load with and without external magnetic perturbation. Nuclear Fusion, 2017, 57, 066045.	3.5	12
180	The role of the density profile in the ASDEX-Upgrade pedestal structure. Plasma Physics and Controlled Fusion, 2017, 59, 014017.	2.1	69

#	Article	IF	CITATIONS
181	Intra-ELM tungsten sputtering in JET ITER-like wall: analytical studies of Be impurity and ELM type influence. Physica Scripta, 2017, T170, 014065.	2.5	3
182	Challenges in the extrapolation from DD to DT plasmas: experimental analysis and theory based predictions for JET-DT. Plasma Physics and Controlled Fusion, 2017, 59, 014023.	2.1	33
183	Impurity re-distribution in the corner regions of the JET divertor. Physica Scripta, 2017, T170, 014060.	2.5	6
184	The near infrared imaging system for the real-time protection of the JET ITER-like wall. Physica Scripta, 2017, T170, 014027.	2.5	8
185	MeV-range velocity-space tomography from gamma-ray and neutron emission spectrometry measurements at JET. Nuclear Fusion, 2017, 57, 056001.	3.5	52
186	Characterization of a compact LaBr ₃ (Ce) detector with Silicon photomultipliers at high 14 MeV neutron fluxes. Journal of Instrumentation, 2017, 12, C10007-C10007.	1.2	8
187	Fine metal dust particles on the wall probes from JET-ILW. Physica Scripta, 2017, T170, 014038.	2.5	22
188	Statistical validation of predictive TRANSP simulations of baseline discharges in preparation for extrapolation to JET D–T. Nuclear Fusion, 2017, 57, 066032.	3.5	11
189	An analytical expression for ion velocities at the wall including the sheath electric field and surface biasing for erosion modeling at JET ILW. Nuclear Materials and Energy, 2017, 12, 341-345.	1.3	10
190	Recent progress towards a quantitative description of filamentary SOL transport. Nuclear Fusion, 2017, 57, 056044.	3.5	56
191	Overview of recent physics results from MAST. Nuclear Fusion, 2017, 57, 102007.	3.5	16
192	Overview of ASDEX Upgrade results. Nuclear Fusion, 2017, 57, 102015.	3.5	53
193	Axisymmetric oscillations at L–H transitions in JET: M-mode. Nuclear Fusion, 2017, 57, 022021.	3.5	29
194	Dimensionless scalings of confinement, heat transport and pedestal stability in JET-ILW and comparison with JET-C. Plasma Physics and Controlled Fusion, 2017, 59, 014014.	2.1	26
195	Impact of toroidal and poloidal mode spectra on the control of non-axisymmetric fields in tokamaks. Physics of Plasmas, 2017, 24, .	1.9	19
196	Tractable flux-driven temperature, density, and rotation profile evolution with the quasilinear gyrokinetic transport model QuaLiKiz. Plasma Physics and Controlled Fusion, 2017, 59, 124005.	2.1	57
197	Heat flux pattern in detached L-modes and ELM mitigated H-modes with rotating magnetic perturbations in ASDEX Upgrade. Nuclear Fusion, 2017, 57, 116006.	3.5	28
198	Synthetic neutron camera and spectrometer in JET based on AFSI-ASCOT simulations. Journal of Instrumentation, 2017, 12, C09010-C09010.	1.2	7

#	Article	IF	CITATIONS
199	Physics and operation oriented activities in preparation of the JT-60SA tokamak exploitation. Nuclear Fusion, 2017, 57, 085001.	3.5	20
200	Axisymmetric global Alfvén eigenmodes within the ellipticity-induced frequency gap in the Joint European Torus. Physics of Plasmas, 2017, 24, .	1.9	16
201	Metallic mirrors for plasma diagnosis in current and future reactors: tests for ITER and DEMO. Physica Scripta, 2017, T170, 014061.	2.5	12
202	First ERO2.0 modeling of Be erosion and non-local transport in JET ITER-like wall. Physica Scripta, 2017, T170, 014018.	2.5	27
203	Analyses of microstructure, composition and retention of hydrogen isotopes in divertor tiles of JET with the ITER-like wall. Physica Scripta, 2017, T170, 014031.	2.5	13
204	Dynamic power balance analysis in JET. Physica Scripta, 2017, T170, 014035.	2.5	2
205	Bayesian electron density inference from JET lithium beam emission spectra using Gaussian processes. Nuclear Fusion, 2017, 57, 036017.	3.5	16
206	Synthetic NPA diagnostic for energetic particles in JET plasmas. Journal of Instrumentation, 2017, 12, C11025-C11025.	1.2	4
207	Self-consistent coupling of DSMC method and SOLPS code for modeling tokamak particle exhaust. Nuclear Fusion, 2017, 57, 066037.	3.5	6
208	Overview of the TCV tokamak program: scientific progress and facility upgrades. Nuclear Fusion, 2017, 57, 102011.	3.5	52
209	Gyrokinetic modeling of impurity peaking in JET H-mode plasmas. Physics of Plasmas, 2017, 24, .	1.9	13
210	Tritium analysis of divertor tiles used in JET ITER-like wall campaigns by means of <i>β</i> -ray induced x-ray spectrometry. Physica Scripta, 2017, T170, 014014.	2.5	6
211	Time-resolved deposition in the remote region of the JET-ILW divertor: measurements and modelling. Physica Scripta, 2017, T170, 014059.	2.5	6
212	The â€~neutron deficit' in the JET tokamak. Nuclear Fusion, 2017, 57, 076029.	3.5	25
213	Edge profile analysis of Joint European Torus (JET) Thomson scattering data: Quantifying the systematic error due to edge localised mode synchronisation. Review of Scientific Instruments, 2016, 87, 013507.	1.3	7
214	Bayesian modelling of the emission spectrum of the Joint European Torus Lithium Beam Emission Spectroscopy system. Review of Scientific Instruments, 2016, 87, 023501.	1.3	10
215	Characterisation of the deuterium recycling at the W divertor target plates in JET during steady-state plasma conditions and ELMs. Physica Scripta, 2016, T167, 014076.	2.5	27
216	Simulating the nitrogen migration in Be/W tokamaks with WallDYN. Physica Scripta, 2016, T167, 014079.	2.5	6

#	Article	IF	CITATIONS
217	Classification of JET Neutron and Gamma Emissivity Profiles. Journal of Instrumentation, 2016, 11, C05021-C05021.	1.2	0
218	Analytical calculations for impurity seeded partially detached divertor conditions. Plasma Physics and Controlled Fusion, 2016, 58, 045013.	2.1	49
219	Core fusion power gain and alpha heating in JET, TFTR, and ITER. Nuclear Fusion, 2016, 56, 056002.	3.5	5
220	Plasma confinement at JET. Plasma Physics and Controlled Fusion, 2016, 58, 014034.	2.1	28
221	Experimental estimation of tungsten impurity sputtering due to Type I ELMs in JET-ITER-like wall using pedestal electron cyclotron emission and target Langmuir probe measurements. Physica Scripta, 2016, T167, 014005.	2.5	31
222	Comparative gyrokinetic analysis of JET baseline H-mode core plasmas with carbon wall and ITER-like wall. Plasma Physics and Controlled Fusion, 2016, 58, 045021.	2.1	3
223	An Analytical Expression for the Electric Field and Particle Tracing in Modelling of Be Erosion Experiments at the JET ITERâ€ike Wall. Contributions To Plasma Physics, 2016, 56, 640-645.	1.1	26
224	High performance detectors for upgraded gamma ray diagnostics for JET DT campaigns. Physica Scripta, 2016, 91, 064003.	2.5	18
225	First neutron spectroscopy measurements with a pixelated diamond detector at JET. Review of Scientific Instruments, 2016, 87, 11D833.	1.3	42
226	Gyrokinetic study of turbulence suppression in a JET-ILW power scan. Plasma Physics and Controlled Fusion, 2016, 58, 115005.	2.1	22
227	MHD marking using the MSE polarimeter optics in ILW JET plasmas. Review of Scientific Instruments, 2016, 87, 11E556.	1.3	0
228	Benchmarking the GENE and GYRO codes through the relative roles of electromagnetic and <i>E</i> — <i>B</i> stabilization in JET high-performance discharges. Plasma Physics and G Fusion, 2016, 58, 125018.	C an trolled	17
229	Deep deuterium retention and Be/W mixing at tungsten coated surfaces in the JET divertor. Physica Scripta, 2016, T167, 014061.	2.5	14
230	JET diagnostic enhancements in preparation for DT operations. Review of Scientific Instruments, 2016, 87, 11D443.	1.3	9
231	Performance of the prototype LaBr3 spectrometer developed for the JET gamma-ray camera upgrade. Review of Scientific Instruments, 2016, 87, 11E717.	1.3	24
232	Gamma-ray spectroscopy at MHz counting rates with a compact LaBr3 detector and silicon photomultipliers for fusion plasma applications. Review of Scientific Instruments, 2016, 87, 11E714.	1.3	31
233	Neutron emission spectroscopy of DT plasmas at enhanced energy resolution with diamond detectors. Review of Scientific Instruments, 2016, 87, 11D822.	1.3	22
234	Response function of single crystal synthetic diamond detectors to 1-4 MeV neutrons for spectroscopy of D plasmas. Review of Scientific Instruments, 2016, 87, 11D823.	1.3	18

#	Article	IF	CITATIONS
235	How to assess the efficiency of synchronization experiments in tokamaks. Nuclear Fusion, 2016, 56, 076008.	3.5	14
236	Scaling of the frequencies of the type one edge localized modes and their effect on the tungsten source in JET ITER-like wall. Plasma Physics and Controlled Fusion, 2016, 58, 125014.	2.1	4
237	Numerical calculations of non-inductive current driven by microwaves in JET. Plasma Physics and Controlled Fusion, 2016, 58, 125001.	2.1	3
238	Experimental investigation of geodesic acoustic modes on JET using Doppler backscattering. Nuclear Fusion, 2016, 56, 106026.	3.5	24
239	JET Tokamak, preparation of a safety case for tritium operations. Fusion Engineering and Design, 2016, 109-111, 1308-1312.	1.9	3
240	Nitrogen retention mechanisms in tokamaks with beryllium and tungsten plasma-facing surfaces. Physica Scripta, 2016, T167, 014077.	2.5	18
241	Neutronic analysis of JET external neutron monitor response. Fusion Engineering and Design, 2016, 109-111, 99-103.	1.9	5
242	The non-thermal origin of the tokamak low-density stability limit. Nuclear Fusion, 2016, 56, 056010.	3.5	5
243	Diagnostic application of magnetic islands rotation in JET. Nuclear Fusion, 2016, 56, 076004.	3.5	12
244	Asymmetric toroidal eddy currents (ATEC) to explain sideways forces at JET. Nuclear Fusion, 2016, 56, 106010.	3.5	23
245	Sparse representation of signals: from astrophysics to real-time data analysis for fusion plasmas and system optimization analysis for ITER and TCV. Plasma Physics and Controlled Fusion, 2016, 58, 123001.	2.1	6
246	The role of MHD in causing impurity peaking in JET hybrid plasmas. Nuclear Fusion, 2016, 56, 066002.	3.5	37
247	Impact of divertor geometry on radiative divertor performance in JET H-mode plasmas. Plasma Physics and Controlled Fusion, 2016, 58, 045011.	2.1	25
248	Stationary Zonal Flows during the Formation of the Edge Transport Barrier in the JET Tokamak. Physical Review Letters, 2016, 116, 065002.	7.8	64
249	Improved ERO modelling for spectroscopy of physically and chemically assisted eroded beryllium from the JET-ILW. Nuclear Materials and Energy, 2016, 9, 604-609.	1.3	17
250	Fast-ion energy resolution by one-step reaction gamma-ray spectrometry. Nuclear Fusion, 2016, 56, 046009.	3.5	31
251	Plasma turbulence measured with fast frequency swept reflectometry in JET H-mode plasmas. Nuclear Fusion, 2016, 56, 126019.	3.5	5
252	Characteristics of pre-ELM structures during ELM control experiment on JET withn  =  2 magnet perturbations. Nuclear Fusion, 2016, 56, 092011.	ic _{3.5}	0

#	Article	IF	CITATIONS
253	Evaluation of reconstruction errors and identification of artefacts for JET gamma and neutron tomography. Review of Scientific Instruments, 2016, 87, 013502.	1.3	6
254	A generalized Abel inversion method for gamma-ray imaging of thermonuclear plasmas. Journal of Instrumentation, 2016, 11, C03001-C03001.	1.2	2
255	COREDIV and SOLPS Numerical Simulations of the Nitrogen Seeded JET ILW Lâ€mode Discharges. Contributions To Plasma Physics, 2016, 56, 760-765.	1.1	6
256	Modelling of the JET DT Experiments in Carbon and ITER-like Wall Configurations. Contributions To Plasma Physics, 2016, 56, 766-771.	1.1	3
257	Effect of PFC Recycling Conditions on JET Pedestal Density. Contributions To Plasma Physics, 2016, 56, 754-759.	1.1	6
258	Experience of handling beryllium, tritium and activated components from JET ITER like wall. Physica Scripta, 2016, T167, 014057.	2.5	18
259	Stabilization of sawteeth with third harmonic deuterium ICRF-accelerated beam in JET plasmas. Physics of Plasmas, 2016, 23, 012505.	1.9	4
260	Tritium distributions on tungsten and carbon tiles used in the JET divertor. Physica Scripta, 2016, T167, 014009.	2.5	10
261	Multi-machine scaling of the main SOL parallel heat flux width in tokamak limiter plasmas. Plasma Physics and Controlled Fusion, 2016, 58, 074005.	2.1	36
262	Thermo-mechanical properties of W/Mo markers coatings deposited on bulk W. Physica Scripta, 2016, T167, 014028.	2.5	2
263	Global optimization driven by genetic algorithms for disruption predictors based on APODIS architecture. Fusion Engineering and Design, 2016, 112, 1014-1018.	1.9	6
264	Characterization of a diamond detector to be used as neutron yield monitor during the in-vessel calibration of JET neutron detectors in preparation of the DT experiment. Fusion Engineering and Design, 2016, 106, 93-98.	1.9	8
265	Neutronics experiments and analyses in preparation of DT operations at JET. Fusion Engineering and Design, 2016, 109-111, 895-905.	1.9	19
266	The role and application of ion beam analysis for studies of plasma-facing components in controlled fusion devices. Nuclear Instruments & Methods in Physics Research B, 2016, 371, 4-11.	1.4	18
267	Non-linear MHD simulations of ELMs in JET and quantitative comparisons to experiments. Plasma Physics and Controlled Fusion, 2016, 58, 014026.	2.1	20
268	Deuterium trapping and release in JET ITER-like wall divertor tiles. Physica Scripta, 2016, T167, 014074.	2.5	20
269	X-ray micro-laminography for the <i>ex situ</i> analysis of W-CFC samples retrieved from JET ITER-like wall. Physica Scripta, 2016, T167, 014050.	2.5	1
270	Erosion and deposition in the JET divertor during the first ILW campaign. Physica Scripta, 2016, T167, 014051.	2.5	58

#	Article	IF	CITATIONS
271	Core turbulent transport in tokamak plasmas: bridging theory and experiment with QuaLiKiz. Plasma Physics and Controlled Fusion, 2016, 58, 014036.	2.1	81
272	Real-time control of ELM and sawtooth frequencies: similarities and differences. Nuclear Fusion, 2016, 56, 016008.	3.5	7
273	Studies of Be migration in the JET tokamak using AMS with 10Be marker. Nuclear Instruments & Methods in Physics Research B, 2016, 371, 370-375.	1.4	12
274	JET experiments with tritium and deuterium–tritium mixtures. Fusion Engineering and Design, 2016, 109-111, 925-936.	1.9	19
275	Deposition in the inner and outer corners of the JET divertor with carbon wall and metallic ITER-like wall. Physica Scripta, 2016, T167, 014052.	2.5	14
276	Numerical study of potential heat flux mitigation effects in the TCV snowflake divertor. Plasma Physics and Controlled Fusion, 2016, 58, 045027.	2.1	27
277	JET experience on managing radioactive waste and implications for ITER. Fusion Engineering and Design, 2016, 109-111, 979-985.	1.9	7
278	Radiation damage and nuclear heating studies in selected functional materials during the JET DT campaign. Fusion Engineering and Design, 2016, 109-111, 1011-1015.	1.9	13
279	Modelling of plasma-edge and plasma–wall interaction physics at JET with the metallic first-wall. Physica Scripta, 2016, T167, 014078.	2.5	2
280	Long-term fuel retention in JET ITER-like wall. Physica Scripta, 2016, T167, 014075.	2.5	52
281	Investigation on the erosion/deposition processes in the ITER-like wall divertor at JET using glow discharge optical emission spectrometry technique. Physica Scripta, 2016, T167, 014049.	2.5	6
282	Advances in understanding and utilising ELM control in JET. Plasma Physics and Controlled Fusion, 2016, 58, 014017.	2.1	7
283	Scaling of the MHD perturbation amplitude required to trigger a disruption and predictions for ITER. Nuclear Fusion, 2016, 56, 026007.	3.5	51
284	Application of transfer entropy to causality detection and synchronization experiments in tokamaks. Nuclear Fusion, 2016, 56, 026006.	3.5	18
285	Raman microscopy investigation of beryllium materials. Physica Scripta, 2016, T167, 014027.	2.5	14
286	Risk Mitigation for ITER by a Prolonged and Joint International Operation of JET. Journal of Fusion Energy, 2016, 35, 85-93.	1.2	4
287	On determining the prediction limits of mathematical models for time series. Journal of Instrumentation, 2016, 11, C07013-C07013.	1.2	1
288	The merits of ion cyclotron resonance heating schemes for sawtooth control in tokamak plasmas. Journal of Plasma Physics, 2015, 81, .	2.1	5

#	Article	IF	CITATIONS
289	Interpretation of radiative divertor studies with impurity seeding in type-I ELMy H-mode plasmas in JET-ILW using EDGE2D–EIRENE. Journal of Nuclear Materials, 2015, 463, 135-142.	2.7	24
290	EMC3-Eirene simulations of particle- and energy fluxes to main chamber- and divertor plasma facing components in ASDEX Upgrade compared to experiments. Journal of Nuclear Materials, 2015, 463, 744-747.	2.7	20
291	Experimental Validation of a Filament Transport Model in Turbulent Magnetized Plasmas. Physical Review Letters, 2015, 115, 215002.	7.8	89
292	Inferring divertor plasma properties from hydrogen Balmer and Paschen series spectroscopy in JET-ILW. Nuclear Fusion, 2015, 55, 123028.	3.5	40
293	Fast ion energy distribution from third harmonic radio frequency heating measured with a single crystal diamond detector at the Joint European Torus. Review of Scientific Instruments, 2015, 86, 103501.	1.3	25
294	Three-dimensional non-linear magnetohydrodynamic modeling of massive gas injection triggered disruptions in JET. Physics of Plasmas, 2015, 22, .	1.9	45
295	Mass spectrometry analysis of the impurity content in N2 seeded discharges in JET-ILW. Journal of Nuclear Materials, 2015, 463, 684-687.	2.7	13
296	The global build-up to intrinsic edge localized mode bursts seen in divertor full flux loops in JET. Physics of Plasmas, 2015, 22, .	1.9	4
297	Formation of the high density front in the inner far SOL at ASDEX Upgrade and JET. Journal of Nuclear Materials, 2015, 463, 541-545.	2.7	57
298	The effect of the Super-X divertor of MAST Upgrade on impurity radiation as modelled by SOLPS. Journal of Nuclear Materials, 2015, 463, 1209-1213.	2.7	9
299	Advances in the physics basis for the European DEMO design. Nuclear Fusion, 2015, 55, 063003.	3.5	122
300	WEST Physics Basis. Nuclear Fusion, 2015, 55, 063017.	3.5	82
301	Trapped electron mode driven electron heat transport in JET: experimental investigation and gyro-kinetic theory validation. Nuclear Fusion, 2015, 55, 113016.	3.5	12
302	First dust study in JET with the ITER-like wall: sampling, analysis and classification. Nuclear Fusion, 2015, 55, 113033.	3.5	51
303	Radiation asymmetries during the thermal quench of massive gas injection disruptions in JET. Nuclear Fusion, 2015, 55, 123027.	3.5	21
304	L to H mode transition: parametric dependencies of the temperature threshold. Nuclear Fusion, 2015, 55, 073015.	3.5	18
305	Transport analysis and modelling of the evolution of hollow density profiles plasmas in JET and implication for ITER. Nuclear Fusion, 2015, 55, 123001.	3.5	33
306	JET and COMPASS asymmetrical disruptions. Nuclear Fusion, 2015, 55, 113006.	3.5	40

#	Article	IF	CITATIONS
307	Dual sightline measurements of MeV range deuterons with neutron and gamma-ray spectroscopy at JET. Nuclear Fusion, 2015, 55, 123026.	3.5	60
308	Studies of the non-axisymmetric plasma boundary displacement in JET in presence of externally applied magnetic field. Plasma Physics and Controlled Fusion, 2015, 57, 104003.	2.1	2
309	Divertor studies in nitrogen induced completely detached H-modes in full tungsten ASDEX Upgrade. Nuclear Fusion, 2015, 55, 033004.	3.5	126
310	Overview of the JET results. Nuclear Fusion, 2015, 55, 104001.	3.5	50
311	On the interpretation of high-resolution x-ray spectra from JET with an ITER-like wall. Journal of Physics B: Atomic, Molecular and Optical Physics, 2015, 48, 144028.	1.5	11
312	Determination of tungsten and molybdenum concentrations from an x-ray range spectrum in JET with the ITER-like wall configuration. Journal of Physics B: Atomic, Molecular and Optical Physics, 2015, 48, 144023.	1.5	22
313	Free boundary equilibrium in 3D tokamaks with toroidal rotation. Nuclear Fusion, 2015, 55, 063032.	3.5	3
314	Neutron streaming along ducts and labyrinths at the JET biological shielding: Effect of concrete composition. Radiation Physics and Chemistry, 2015, 116, 359-364.	2.8	11
315	Key impact of finite-beta and fast ions in core and edge tokamak regions for the transition to advanced scenarios. Nuclear Fusion, 2015, 55, 053007.	3.5	56
316	Density limit of H-mode plasmas on JET-ILW. Journal of Nuclear Materials, 2015, 463, 445-449.	2.7	10
317	Beryllium migration in JET ITER-like wall plasmas. Nuclear Fusion, 2015, 55, 063021.	3.5	83
318	Turbulent transport analysis of JET H-mode and hybrid plasmas using QuaLiKiz and Trapped Gyro Landau Fluid. Plasma Physics and Controlled Fusion, 2015, 57, 035003.	2.1	7
319	High density operation for reactor-relevant power exhaust. Journal of Nuclear Materials, 2015, 463, 22-29.	2.7	97
320	Implications of high density operation on SOL transport: A multimachine investigation. Journal of Nuclear Materials, 2015, 463, 123-127.	2.7	31
321	WALLDYN simulations of global impurity migration in JET and extrapolations to ITER. Nuclear Fusion, 2015, 55, 053015.	3.5	67
322	Plasma isotopic changeover experiments in JET under carbon and ITER-like wall conditions. Nuclear Fusion, 2015, 55, 043021.	3.5	8
323	Benchmark experiments on neutron streaming through JET Torus Hall penetrations. Nuclear Fusion, 2015, 55, 053028.	3.5	29
324	Comparative analysis of core heat transport of JET high density H-mode plasmas in carbon wall and ITER-like wall. Plasma Physics and Controlled Fusion, 2015, 57, 065002.	2.1	6

#	Article	IF	CITATIONS
325	Experimental investigation of neon seeding in the snowflake configuration in TCV. Journal of Nuclear Materials, 2015, 463, 1196-1199.	2.7	9
326	Model-based radiation scalings for the ITER-like divertors of JET and ASDEX Upgrade. Journal of Nuclear Materials, 2015, 463, 546-550.	2.7	9
327	Integrated core–SOL–divertor modelling for ITER including impurity: effect of tungsten on fusion performance in H-mode and hybrid scenario. Nuclear Fusion, 2015, 55, 053032.	3.5	6
328	Partial detachment of high power discharges in ASDEX Upgrade. Nuclear Fusion, 2015, 55, 053026.	3.5	163
329	Recent ASDEX Upgrade research in support of ITER and DEMO. Nuclear Fusion, 2015, 55, 104010.	3.5	16
330	Improved confinement in JET highβplasmas with an ITER-like wall. Nuclear Fusion, 2015, 55, 053031.	3.5	79
331	The impact of poloidal asymmetries on tungsten transport in the core of JET H-mode plasmas. Physics of Plasmas, 2015, 22, 055902.	1.9	49
332	Physics of Plasmas, 2015, 22, 056115.	1.9	37
333	Influence of theE  ×  Bdrift in high recycling divertors on target asymmetries. Plasma Physics a Controlled Fusion, 2015, 57, 095002.	and 2.1	56
334	Ion target impact energy during Type I edge localized modes in JET ITER-like Wall. Plasma Physics and Controlled Fusion, 2015, 57, 085006.	2.1	44
335	Experimental studies and modeling of complete H-mode divertor detachment in ASDEX Upgrade. Journal of Nuclear Materials, 2015, 463, 128-134.	2.7	71
336	Scaling of the divertor power spreading (S-factor) in open and closed divertor operation in JET and ASDEX Upgrade. Journal of Nuclear Materials, 2015, 463, 49-54.	2.7	30
337	SOLPS analysis of the MAST-U divertor with the effect of heating power and pumping on the access to detachment in the Super-x configuration. Plasma Physics and Controlled Fusion, 2015, 57, 115001.	2.1	40
338	Experimental evaluation of stable long term operation of semiconductor magnetic sensors at ITER relevant environment. Nuclear Fusion, 2015, 55, 083006.	3.5	21
339	Numerical simulations of JET discharges with the ITER-like wall for different nitrogen seeding scenarios. Journal of Nuclear Materials, 2015, 463, 577-581.	2.7	11
340	Contrasting H-mode behaviour with deuterium fuelling and nitrogen seeding in the all-carbon and metallic versions of JET. Nuclear Fusion, 2014, 54, 073016.	3.5	37
341	A new experimental classification of divertor detachment in ASDEX Upgrade. Nuclear Fusion, 2014, 54, 013001.	3.5	118
342	Electron density determination in the divertor volume of ASDEX Upgrade via Stark broadening of the Balmer lines. Plasma Physics and Controlled Fusion, 2014, 56, 025010.	2.1	30

#	Article	lF	CITATIONS
343	An experimental investigation of the high density transition of the scrape-off layer transport in ASDEX Upgrade. Nuclear Fusion, 2014, 54, 123005.	3.5	106
344	Investigation of conventional and Super-X divertor configurations of MAST Upgrade using scrape-off layer plasma simulation. Plasma Physics and Controlled Fusion, 2014, 56, 075008.	2.1	19
345	First EMC3-Eirene simulations of the TCV snowflake divertor. Plasma Physics and Controlled Fusion, 2014, 56, 035009.	2.1	34
346	Modelling the Effect of the Super-X Divertor in MAST Upgrade on Transition to Detachment and Distribution of Volumetric Power Losses. Contributions To Plasma Physics, 2014, 54, 448-453.	1.1	9
347	Influence of atomic physics on EDGE2D-EIRENE simulations of JET divertor detachment with carbon and beryllium/tungsten plasma-facing components. Nuclear Fusion, 2014, 54, 093012.	3.5	35
348	DEMO divertor limitations during and in between ELMs. Nuclear Fusion, 2014, 54, 114003.	3.5	107
349	EDGE2D-EIRENE modelling of divertor detachment in JET high triangularity L-mode plasmas in carbon and Be/W environment. Journal of Nuclear Materials, 2013, 438, S638-S642.	2.7	9
350	Overview of the JET results with the ITER-like wall. Nuclear Fusion, 2013, 53, 104002.	3.5	70
351	Overview on plasma operation with a full tungsten wall in ASDEX Upgrade. Journal of Nuclear Materials, 2013, 438, S34-S41.	2.7	156
352	Impact of the ITER-like wall on divertor detachment and on the density limit in the JET tokamak. Journal of Nuclear Materials, 2013, 438, S139-S147.	2.7	76
353	Numerical studies of effects associated with the Super-X divertor on target parameters in MAST-U. Journal of Nuclear Materials, 2013, 438, S545-S549.	2.7	14
354	Characterization of the fluctuating detachment state in ASDEX Upgrade. Journal of Nuclear Materials, 2013, 438, S285-S290.	2.7	38
355	Design and concept validation of the new solid tungsten divertor for ASDEX Upgrade. Fusion Engineering and Design, 2013, 88, 577-580.	1.9	12
356	L-mode radiative plasma edge studies for model validation in ASDEX Upgrade and JET. Journal of Nuclear Materials, 2013, 438, S321-S325.	2.7	17
357	Overview of ASDEX Upgrade results. Nuclear Fusion, 2013, 53, 104003.	3.5	36
358	On the physics guidelines for a tokamak DEMO. Nuclear Fusion, 2013, 53, 073019.	3.5	192
359	Impurity seeding for tokamak power exhaust: from present devices via ITER to DEMO. Plasma Physics and Controlled Fusion, 2013, 55, 124041.	2.1	303
360	Benchmarking of a 1D scrape-off layer code SOLF1D with SOLPS and its use in modelling long-legged divertors. Plasma Physics and Controlled Fusion, 2013, 55, 065004.	2.1	15

#	Article	IF	CITATIONS
361	Outer divertor of ASDEX Upgrade in low-density L-mode discharges in forward and reversed magnetic field: II. Analysis of local impurity migration. Nuclear Fusion, 2012, 52, 103007.	3.5	7
362	Outer divertor of ASDEX Upgrade in low-density L-mode discharges in forward and reversed magnetic field: I. Comparison between measured plasma conditions and SOLPS5.0 code calculations. Nuclear Fusion, 2012, 52, 103006.	3.5	23
363	Influence of cross-field drifts and chemical sputtering on simulations of divertor particle and heat loads in ohmic and L-mode plasmas in DIII-D, AUC, and JET using UEDGE. Journal of Nuclear Materials, 2011, 415, S530-S534.	2.7	21
364	Effect of E×B driven transport on the deposition of carbon in the outer divertor of ASDEX Upgrade. Journal of Nuclear Materials, 2011, 415, S231-S234.	2.7	12
365	3D modeling of the ASDEX Upgrade edge plasma exposed to a localized tungsten source by means of EMC3-Eirene. Journal of Nuclear Materials, 2011, 415, S505-S508.	2.7	15
366	Relevance of collisionality in the transport model assumptions for divertor detachment multi-fluid modelling on JET. Journal of Nuclear Materials, 2011, 415, S535-S539.	2.7	21
367	Assessment of edge modeling in support of ITER. Journal of Nuclear Materials, 2011, 415, S523-S529.	2.7	44
368	Overview of ASDEX Upgrade results. Nuclear Fusion, 2011, 51, 094012.	3.5	27
369	Poloidal distribution of recycling sources and core plasma fueling in DIII-D, ASDEX-Upgrade and JET L-mode plasmas. Plasma Physics and Controlled Fusion, 2011, 53, 124017.	2.1	22
370	EMC3-Eirene simulations of the spatial dependence of the tungsten divertor retention in ASDEX Upgrade. Plasma Physics and Controlled Fusion, 2011, 53, 125010.	2.1	28
371	Overview of JET results. Nuclear Fusion, 2011, 51, 094008.	3.5	33
372	Modelling of Carbon Transport in the Outer Divertor Plasma of ASDEX Upgrade. Contributions To Plasma Physics, 2010, 50, 439-444.	1.1	6
373	Addendum to papers from Axially Symmetric Divertor Experiment (ASDEX) Upgrade Team, published in Review of Scientific Instruments. Review of Scientific Instruments, 2010, 81, 039903.	1.3	Ο
374	Overview of ASDEX Upgrade results. Nuclear Fusion, 2009, 49, 104009.	3.5	11
375	Simulation of ASDEX Upgrade Ohmic plasmas for SOLPS code validation. Nuclear Fusion, 2009, 49, 015004.	3.5	18
376	Measurements of neutral gas fluxes under different plasma and divertor regimes in ASDEX Upgrade. Journal of Nuclear Materials, 2009, 390-391, 494-497.	2.7	24
377	Investigation of local carbon transport in the ASDEX Upgrade divertor using 13CH4 puffing. Journal of Nuclear Materials, 2009, 390-391, 68-71.	2.7	15
378	Current understanding of divertor detachment: Experiments and modelling. Journal of Nuclear Materials, 2009, 390-391, 250-254.	2.7	50

#	Article	IF	CITATIONS
379	Pressure balance between midplane and inner and outer divertor in ASDEX Upgrade H-mode discharges. Journal of Nuclear Materials, 2009, 390-391, 278-281.	2.7	0
380	Integrated modelling of ITER reference scenarios. Nuclear Fusion, 2009, 49, 075030.	3.5	50
381	Modelling of13CH4injection and local carbon deposition at the outer divertor of ASDEX Upgrade. Physica Scripta, 2009, T138, 014019.	2.5	7
382	Progress in Edge Plasma Transport Modeling on JET. Contributions To Plasma Physics, 2008, 48, 190-195.	1.1	3
383	Simulating the Role of Intrinsic Carbon Impurities in the Divertor Detachment of ASDEX Upgrade. Contributions To Plasma Physics, 2008, 48, 249-254.	1.1	15
384	Divertor power and particle fluxes between and during type-I ELMs in the ASDEX Upgrade. Nuclear Fusion, 2008, 48, 085008.	3.5	35
385	Discrepancy between modelled and measured radial electric fields in the scrape-off layer of divertor tokamaks: a challenge for 2D fluid codes?. Nuclear Fusion, 2007, 47, 479-489.	3.5	38
386	Divertor plasma flow near the lower x-point in ASDEX Upgrade. Plasma Physics and Controlled Fusion, 2007, 49, 857-872.	2.1	17
387	A possible role of radial electric field in driving parallel ion flow in scrape-off layer of divertor tokamaks. Nuclear Fusion, 2007, 47, 762-772.	3.5	39
388	Plasma wall interaction and its implication in an all tungsten divertor tokamak. Plasma Physics and Controlled Fusion, 2007, 49, B59-B70.	2.1	110
389	Parallel SOL flow on TCV. Journal of Nuclear Materials, 2007, 363-365, 505-510.	2.7	59
390	High recycling outer divertor regimes after type-I ELMs at high density in ASDEX Upgrade. Journal of Nuclear Materials, 2007, 363-365, 448-452.	2.7	15
391	Radiation distributions in TCV. Journal of Nuclear Materials, 2007, 363-365, 1104-1109.	2.7	7
392	SOLPS5 modelling of the type III ELMing H-mode on TCV. Journal of Nuclear Materials, 2007, 363-365, 1037-1043.	2.7	11
393	Safety factor profile requirements for electron ITB formation in TCV. Plasma Physics and Controlled Fusion, 2005, 47, B107-B120.	2.1	22
394	AXUV bolometer and Lyman-Î \pm camera systems on the TCV tokamak. Review of Scientific Instruments, 2004, 75, 4139-4141.	1.3	16
395	Divertor modelling of septum assessment experiments in JET MkIIGB. Contributions To Plasma Physics, 2004, 44, 241-246.	1.1	2
396	The influence of molecular dynamics on divertor detachment in TCV. Contributions To Plasma Physics, 2004, 44, 268-273.	1.1	14

#	Article	IF	CITATIONS
397	Divertor detachment during pure helium plasmas in JET. Journal of Nuclear Materials, 2003, 313-316, 980-985.	2.7	13
398	An overview of JET edge modelling activities. Journal of Nuclear Materials, 2003, 313-316, 868-872.	2.7	10
399	An overview of results from the TCV tokamak. Nuclear Fusion, 2003, 43, 1619-1631.	3.5	25
400	Recent results from the electron cyclotron heated plasmas in Tokamak à Configuration Variable (TCV). Physics of Plasmas, 2003, 10, 1796-1802.	1.9	26
401	Overview of JET results. Nuclear Fusion, 2003, 43, 1540-1554.	3.5	38
402	Accessibility and properties of ELMy H-mode and ITB plasmas in TCV. Plasma Physics and Controlled Fusion, 2003, 45, A351-A365.	2.1	13
403	ECH physics and new operational regimes on TCV. Plasma Physics and Controlled Fusion, 2002, 44, B85-B97.	2.1	5